Journal of Rock Mechanics and Geotechnical Engineering 15 (2023) 500–509

Contents lists available at ScienceDirect

Journal of Rock Mechanics and Geotechnical Engineering

journal homepage: www.jrmge.cn

Full Length Article

Geotechnical investigation of low-plasticity organic soil treated with nano-calcium carbonate

Govindarajan Kannan [a], Brendan C. O'Kelly [b], Evangelin Ramani Sujatha [a,*]

[a] Centre for Advanced Research in Environment, School of Civil Engineering, SASTRA Deemed to be University, Thanjavur, Tamil Nadu, 613401, India
[b] Department of Civil, Structural and Environmental Engineering, Trinity College Dublin, Dublin, D02 PN40, Ireland

ARTICLE INFO

Article history:
Received 6 October 2021
Received in revised form
29 April 2022
Accepted 15 May 2022
Available online 7 June 2022

Keywords:
Organic silt
Calcium carbonate
Nano-calcium carbonate (NCC)
Calcium silicate hydrate (CSH)
Soil stabilization

ABSTRACT

Soil stabilization using nanomaterials is an emerging research area although, to date, its investigation has mostly been laboratory-based and therefore requires extensive study for transfer to practical field applications. The present study advocates nano-calcium carbonate (NCC) material, a relatively unexplored nanomaterial additive, for stabilization of low-plasticity fine-grained soil having moderate organic content. The plasticity index, compaction, unconfined compressive strength (UCS), compressibility and permeability characteristics of the 0.2%, 0.4%, 0.6% and 0.8% NCC-treated soil, and untreated soil (as control), were determined, including investigations of the effect of up to 90-d curing on the UCS and permeability properties. In terms of UCS improvement, 0.4% NCC addition was identified as the optimum dosage, mobilizing a UCS at 90-d curing of almost twice that for the untreated soil. For treated soil, particle aggregation arising from NCC addition initially produced an increase in the permeability coefficient, but its magnitude decreased for increased curing owing to calcium silicate hydrate (CSH) gel formation, although still remaining higher compared to the untreated soil for all dosages and curing periods investigated. Compression index decreased for all NCC-treated soil investigated. SEM micrographs indicated the presence of gel patches along with particle aggregation. X-ray diffraction (XRD) results showed the presence of hydration products, such as CSH. Significant increases in UCS are initially attributed to void filling and then because of CSH gel formation with increased curing.

1. Introduction

Strength improvement of weak and unsuitable soils for construction activities dates back to ancient times. Ground improvement approaches can involve a variety of techniques, such as soil replacement, conventional methods of soil compaction, installation of stone columns to densify the ground and/or to act as preferential load-bearing elements, accelerated consolidation techniques (e.g. surcharging and/or vacuum consolidation with vertical drains in situ) for reduction of in-service settlements, admixing the existing soil with suitable additive(s) for strength enhancement, and laying of geosynthetics for layer separation, filtration and/or soil reinforcement purposes. Despite numerous established solutions, the research and development of ground improvement techniques remain an emerging field.

Among the many methods described above, admixing the soil with suitable additive(s) is one of the most prevalent techniques used in ground improvement practice. Although cement stabilization gives better performance in terms of the resulting strength and compressibility characteristics, there are serious environmental impacts associated with cement manufacturing (Park et al., 2014). Lime treatment of soil produces a remarkable improvement for clayey soils (Baldovino et al., 2018), but the production of lime from limestone also adversely affects the environment by emission of CO_2 (Gutiérrez et al., 2012). Furthermore, lime carbonation would be an undesirable chemical reaction for lime-treated soil (Kannan et al., 2020). In line with such additives, limestone (as a source of calcium carbonate ($CaCO_3$)) has proved itself as a better strength enhancing agent. For instance, Pastor et al. (2019) investigated the geotechnical behavioral changes for addition of limestone powder (derived from the stone industry) to low-plasticity clay. Results revealed that unconfined compressive strength (UCS) increased to a maximum of 1.48 times that of the untreated soil for addition of

* Corresponding author.
E-mail addresses: r.evangelin@gmail.com, sujatha@civil.sastra.edu (E.R. Sujatha).
Peer review under responsibility of Institute of Rock and Soil Mechanics, Chinese Academy of Sciences.

https://doi.org/10.1016/j.jrmge.2022.05.004

25% limestone powder (dry soil mass basis). Further, these authors suggested the feasible reaction between the calcium ions of the additive with the silica or alumina ions of the soil causing the formation of cementitious products, like calcium silicate hydrate (CSH), calcium aluminate hydrate (CAH) and calcium aluminum silicate hydrate (CASH). Ibrahim et al. (2020) used limestone powder for the strength enhancement of a high-plasticity clay obtained from Erbil city in Iraq. Strength and stiffness improved for all investigated dosages. It was found that up to a dosage of 12%, the limestone powder addition slightly reduced the initial void ratio of the compacted soil–limestone powder mixture, with no extra influence evident for higher dosages. Furthermore, addition of limestone powder did not show significant influence on the compressibility characteristics of the soil. Bazarbekova et al. (2021) replaced cement with dosages of limestone powder for strength improvement of silty sand containing considerable sulfate and saline contents. Results revealed that soil treated with 6% cement and 2% limestone powder produced a strength improvement of 12 times greater than the untreated strength for 28-d curing.

With similar trends, numerous researchers have also investigated calcium carbonate produced through microbial actions, as an initiative towards environmental-friendly approaches to synthesize $CaCO_3$ for ground improvement applications (Carmona et al., 2018). Various methods have been investigated for producing the microbial-induced calcite precipitation (MICP), like urea hydrolysis, denitrification, and sulfate reduction (Shahrokhi-Shahraki et al., 2015; Amin et al., 2017; Rahman et al., 2020; Assadi-Langroudi et al., 2022). However, urea hydrolysis (involving precipitation of $CaCO_3$ using urease enzyme, urea and $CaCl_2$) remains the most common technique, owing to its higher efficiency and easy control (Rahman et al., 2020). Kannan et al. (2020) investigated 0.5 mol MICP-treated high-plasticity marine clays and they found a maximum improvement in the undrained shear strength of 1.48 times and a reduction in the compressibility of 32% for the treated soil. Konstantinou et al. (2021) investigated the strength of MICP-treated fine and coarse sands, with the treated sands mobilizing strengths comparable to soft carbonate sandstones. Moreover, the strength was higher for the treated fine sand, as the void size in the coarse sand was greater than that of the $CaCO_3$ crystals. Morales et al. (2019) studied the effects of MICP treatment on clay phyllites, reporting improved strength (in terms of increased friction angle) and reduced compressibility. However, they observed an important constraint, in that compacting the samples post-treatment hindered the binding effect created through cementation and also reduced the maximum dry density achieved. Mujah et al. (2019) established a method to estimate the amount of $CaCO_3$ produced via MICP precipitation. They also found that the strength of sand treated with 10% $CaCO_3$ produced via MICP was 36.67% greater than that achieved for ordinary Portland-cement-treated samples. Several other recently published articles also highlighted the advantages of using MICP for soil treatment (Shahrokhi-Shahraki et al., 2015; Amin et al., 2017; Zomorodian et al., 2019b; Choi et al., 2020; Rahman et al., 2020; Soundara et al., 2020). The basic mechanisms of strength improvement achieved by the MICP treatment method are bio-cementation (binding of soil particles together via inorganic bio-cement) and bio-clogging (filling of pore voids using the bio-cement) (Soundara et al., 2020; Assadi-Langroudi et al., 2022). However, this method highly relies on the nature of the soil, bacteria and environmental conditions (i.e. soil type, bacterial concentration, cementing solution type, and pH value) for better performance (Zhao et al., 2014; Shahrokhi-Shahraki et al., 2015; Zomorodian et al., 2019b; Soundara et al., 2020; Assadi-Langroudi et al., 2022). For instance, Cardoso et al. (2018) analyzed sand and sand–kaolin combinations with MICP treatment. Results from their study indicated that MICP showed a complex relationship due to the presence of clay minerals in the sand–kaolin combinations. Hence, before opting for this treatment method, a detailed investigation concerning the clay minerals present in the soil is mandatory (Cardoso et al., 2018). Critically, this method is most suitable for soils with constituent particle sizes ranging between 50 μm and 400 μm (Rebata-Landa, 2007; Soundara et al., 2020), so as to achieve easy permeation of the bacterial cell solution, which may not be attainable for all situations. In this regard, the practical suitability of the MICP method must consider the required soil treatment depth (Assadi-Langroudi et al., 2022). In addition, higher dosages are required to stabilize the soil using limestone powder addition and the MICP treatment combination, underlining the need to find a suitable soil additive that can achieve appreciable strength gain for a relatively smaller dosage.

A trending technology in soil stabilization over the past decade is to stabilize the soil using nanomaterials. These are materials whose constituent particles have one of their dimensions ranging between 1 nm and 100 nm (Kannan and Sujatha, 2021). Nanomaterials are produced by the top-down method (i.e. reducing the size of large particles to create smaller ones), or by the bottom-up method that involves chemical synthesis by building up sub-nano-sized materials (Rahman and Padavettan, 2012). Studies on nano-sized materials showed enhanced geotechnical engineering performance compared to their micro-sized counterparts. For instance, Wu et al. (2017) reported that nano-silica (NS) showed enhanced pozzolanic activity and hydration reaction when blended with cement compared to micro-sized silica. Khalid et al. (2015) stated that converting micro to nano (clay) makes the soil susceptible to more significant interaction/reaction during the conversion. This modification occurs since nanomaterials tend to possess higher specific surface area, higher surface activity (Cao and Wang, 2018) and greater cation exchange capacity (Majeed and Taha, 2013). Mohammadi et al. (2021, 2022) observed that with decreasing particle size to nanoscale, the quantity of additive required to achieve optimum geomechanical performance also decreased.

Changizi and Haddad (2017) stabilized soft clay using NS additive and, relative to the untreated soil, they found a strength improvement of 1.56 times achieved for a low dosage of 0.7% NS. Ali Zomorodian et al. (2017) investigated the strength improvement of loess using nano-clay material and found a strength improvement of 3.75 times achieved for 1% nano-clay addition. Emmanuel et al. (2019) studied the advantages of using 5% halloysite nanotubes for marine clay stabilization. Results showed that halloysite nanotube addition improved the strength by a minimum of 1.51 times for 14-d curing. Alsharef et al. (2020) studied the effects of carbon nanotube and carbon nanofiber additions for various clayey soils. Carbon nanotubes showed minimum UCS improvements of 2 times for low-plasticity clays and of 1.32 times for high-plasticity clays, while carbon nanofibers showed UCS improvements of 2.38 times for low-plasticity clays and of 1.54 times for high-plasticity clays (Alsharef et al., 2020). Choobbasti et al. (2019) attempted to stabilize low-plasticity clay with carpet waste fibers and nano-calcium carbonate (NCC) material. As part of their investigation, they studied the UCS of NCC-treated soil and reported a 100% strength improvement for a 1.2% dosage at 42-d curing. Mohammadi et al. (2021, 2022) investigated the strength enhancement achieved for NCC-treated clayey sand comprising different combinations of bentonite and kaolinite in the soil. They reported the formation of CSH gel in the treated soil on account of the high reactive behavior of the NCC material.

A thorough survey of the pertinent literature shows that nanomaterials are highly effective in improving the strength of soil (Ghasabkolaei et al., 2017). Several researchers have used NS and nano-clay additives to enhance the soil geotechnical properties, making them the most commonly used nanomaterials for soil

stabilization purposes (Taha and Taha, 2012; Ali Zomorodian et al., 2017; Changizi and Haddad, 2017; Ahmadi and Shafiee, 2019; Zomorodian et al., 2019a, 2020). However, studies have pointed out that the effectiveness of these nanomaterials in soil stabilization depends to a considerable extent on the soil type (Taha and Taha, 2012), as well as other influencing parameters. Choobbasti et al. (2019) studied the efficacy of NCC material as a secondary additive with carpet waste fibers and reported encouraging results. Mohammadi et al. (2021, 2022) showed that NCC has the potential to react with the minerals in the soil leading to strength improvement. However, to date, research investigations reporting on NCC-treated soil are sparse and only consider selection of soil types, like clayey sand and low compressible clay.

The present study recommends the use of NCC material as a unary additive for stabilizing a regionally problematic soil (low-plasticity silt with organic content) from assessments of the improvements achieved in its plasticity, UCS, compressibility and permeability characteristics. The mechanism of stabilization was identified using scanning electron microscope (SEM), Fourier-transform infrared (FTIR) spectroscopy, and X-ray diffraction (XRD) analyses. Curing period is an important factor influencing the resulting geomechanical properties of treated soils. To examine its effect, the geotechnical laboratory testing investigated samples cured for up to 90-d (compared to the 28-d curing period usually employed by researchers). Extrapolation of the experimental data gathered for up to 90-d curing may be useful in deducing properties of the treated soil for longer curing periods ($>>$ 90 d). Furthermore, this study aims to propose NCC material as a viable soil stabilization additive from the viewpoint of reduced additive requirements compared to conventional soil additives.

2. Materials and methods

2.1. Materials

Soil was collected from the cultivation lands in the Ariyalur district of Tamil Nadu, India. As a regionally problematic soil (low plastic silt with moderate organic content), this study investigates its improvement using a relatively unexplored nanomaterial (i.e. NCC) towards addressing geotechnical issues associated with these soil deposits for infrastructure development in a region nearby. Usually, soil with organic content exhibits reduced strength and has poor drainage characteristics. The test soil was sampled from a depth of 1 m to avoid the loose topsoil layer and agricultural waste that are not characteristic of the subsoil. The NCC material investigated was purchased from Intelligent Materials Pvt. Ltd., India.

2.2. Methodology

Based on the results of trial studies and from the dosage ranges examined in previous research (Choobbasti et al., 2019), the additive range investigated for this study was set between 0.2% and 0.8%. In other words, the experimental testing was performed for soil treated with 0.2%, 0.4%, 0.6% and 0.8% of NCC additive. To prepare the amended soil, the sampled soil was oven dried and then subdivided into small quantities to which the NCC material of desired dosage (based on the dry soil mass) was added to produce a homogeneous mixture. The small quantities were then combined and mixed thoroughly until uniformity was ensured.

Preliminary tests were performed on the sampled soil, such as particle-size analysis (ASTM D6913/D6913M-17, 2017; ASTM D7928-21e1, 2021), specific gravity of solids (ASTM D854-14, 2014), differential free-swell index (IS2720-40, 1997; ASTM D5890-19, 2019), and organic matter content (ASTM D2974-20, 2020). Standard Proctor (SP) compaction testing was conducted in accordance with ASTM D698-12 (2012) to determine the maximum dry unit weight (MDUW) and corresponding optimum moisture content (OMC) of the untreated and NCC-treated soils. Preliminary compaction studies on the untreated soil showed an OMC of 17.5%. Hence, all compaction tests started with 10% water content, adding the required amount of water to the dry disaggregated, untreated and NCC-treated soils. In order to promote reaction between the additive and soil matrix, the wetted soil–NCC blends were allowed to stand undisturbed for a 12-h period in airlock containers before commencing the compaction testing. The plasticity index was calculated for all dosages based on the results of liquid limit and plastic limit testing (ASTM D4318-17, 2017). A series of test specimens, each 38 mm in diameter by 76 mm in height, was prepared at a moisture content corresponding to the SP MDUW for UCS determinations at different curing periods using unconfined compression tests performed in accordance with ASTM D2166/D2166M-16 (2016). These tests were initially conducted 2 h after sample preparation and then for curing periods of 7 d, 14 d, 28 d, 56 d and 90 d. The test specimens were stored in airlock containers during curing to prevent moisture loss. Similarly, the permeability coefficient of fully saturated NCC-treated soil (SP-compacted at OMC to achieve MDUW) was measured for 7-d, 14-d, 28-d, 56-d and 90-d curing, employing the falling-head method (ASTM D5856-15, 2015). Consolidation testing was performed in accordance with ASTM D2435/D2435M-11(2020) (2020) on untreated soil and for soil treated with 0.2%, 0.4% and 0.6% of NCC to examine the effect of the additive on the compressibility behavior. These samples were cured for 24 h prior to the application of the first load increment. For the tests, the specimens of 60 mm in diameter by initially 20 mm in height were compressed under an applied vertical stress range of 9.8–313.8 kPa, each maintained load stage of 24-h duration.

The mechanism of strength improvement for NCC addition was visually interpreted using the micrographs obtained using an SEM apparatus (Vega 3 Tescan model). The chemical interaction and variations in the NCC-treated soil were ascertained from interpretation of the XRD and FTIR analyses. The XRD analysis was performed for a 2θ range of 20°–80° using a Bruker X-ray diffractometer apparatus. The FTIR investigation was performed for wavenumbers ranging from 4000 cm^{-1} to 400 cm^{-1} using a PerkinElmer spectrometer (Avio, 2000 model).

The porosity of the untreated and NCC-treated soils was estimated using an image-processing technique, whereby the obtained SEM images were processed using the MATLAB R2020b software (Rabbani and Salehi, 2017; Ezeakacha et al., 2018). The principle of this technique is that the original image is subjected to intensity mapping for detection of the pore spaces, followed by binary segmentation involving representation of the pore spaces as a dark shade in white background, and finally the segmentation of the pores using different color identification. Fig. 1 demonstrates the stages in the image processing analysis.

2.3. Material characterization

The sampled soil was black in color, and it was classified as organic soil with low compressibility (OL) according to the unified soil classification system (USCS). The gradation curve, shown in Fig. 2, indicates that the soil consists of 2% gravel, 25% sand, 52% silt and 21% clay.

Some index/geotechnical properties of the test soil are listed in Table 1. The sampled soil had a natural water content of 12%. The specific gravity of its solids of 2.33 was relatively low on account of the 13.6% organic material present. The soil exhibited a high plastic nature and, with a differential free-swell index of 35%, it has a tendency to swell moderately. The SP MDUW and OMC values of the soil corroborate with its high fines content (at 73%).

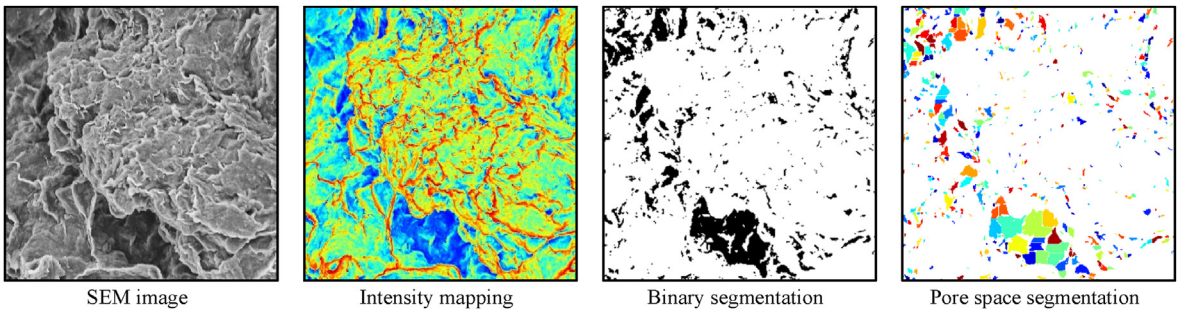

Fig. 1. Sequential stages of image-processing analysis for porosity identification.

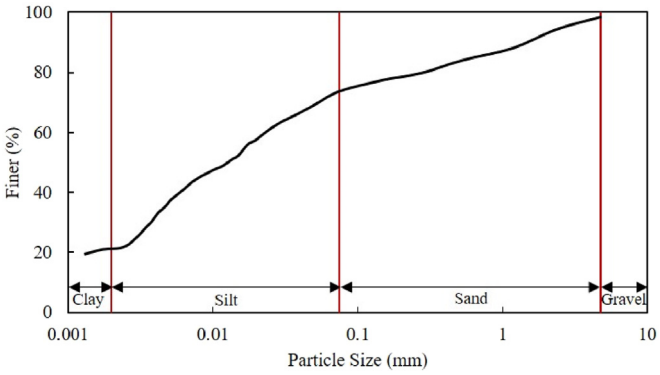

Fig. 2. Grain-size distribution plot for the test soil.

Table 1
Properties of the test soil.

Property	Value
Liquid limit (%)	48.8
Plastic limit (%)	25.9
Plasticity index (%)	22.9
Specific gravity of solids	2.33
Differential free-swell index (%)	35
Organic content (%)	13.6
USCS classification	OL (organic silt)
MDUW (kN/m^3)	16.8
OMC (%)	17.5

Table 2 lists the supplier specifications of the NCC material investigated. It had an average particle size of less than 100 nm, with the bulk density of the material in the range of 300 kg/m^3 to 1400 kg/m^3 (i.e. significantly lower than the density of $CaCO_3$ (2700 kg/m^3)).

The NCC material was 99.9% pure, with negligible metal impurities content of 850 parts per million (ppm). XRD peaks of the material (measured at room temperature) are shown in Fig. 3. The peaks correspond to calcium carbonate mineral and calcite, a polymorph of calcium carbonate.

3. Results and discussion

3.1. Plasticity index

As depicted in Fig. 4, with respective initial values of 48.8%, 25.9% and 22.9% (i.e. for 0% NCC), the liquid limit, plastic limit and plasticity index all increased marginally with increasing additive content, reaching respective values of 53.6%, 27.9% and 25.7% for the highest NCC dosage of 0.8% investigated. The plasticity index values of the treated soil are 24.4%, 25.1%, 25.4% and 25.7% for NCC dosages of 0.2%, 0.4%, 0.6% and 0.8%, respectively.

Table 2
Properties of the investigated NCC material.

Property	Value
Average particle size (nm)	<100
Purity (%)	99.9
Molecular weight (g/mol)	100.08
Color	White
Bulk density (kg/m^3)	300–1400
Melting point (°C)	825
pH value	8–9

The marginal increase in plasticity observed could be because the thorough remolding of the wetted NCC-treated soil mass during the experimental procedure (for performing the consistency limits testing) would have hindered the reaction among the nanoparticles and the soil solids. In other words, for these tests, the NCC additive merely had the effect of modestly increasing the clay-sized fraction of the mixtures (by between an additional 0.2%–0.8%), explaining the slight increase observed in the consistency limits of the treated soil for increasing NCC content. Zhang (2007) suggested that stronger interparticle aggregation caused by the nanomaterial additive means that the water in the pore spaces will not easily dissipate when remolding the soil during the consistency limits testing procedure. This causes an increase in the consistency limits values for the NCC-treated soil.

3.2. Compaction characteristics

Compaction tests conducted on the NCC-treated samples indicated moderate decreases in both OMC and MDUW (Fig. 5), i.e. the untreated soil had an MDUW of 16.8 kN/m^3, reducing to 16.35 kN/m^3, 16.1 kN/m^3, 16.05 kN/m^3 and 16 kN/m^3 for 0.2%, 0.4%, 0.6% and 0.8% NCC addition, respectively. Untreated soil had an OMC of 17.5%, reducing to between 14.2% and 14.3% water content for 0.2%–0.8% NCC addition.

The reduction in both MDUW and OMC with increasing NCC content is the typical behavior of low-plasticity organic silt. A plausible reason for the decreases in MDUW and OMC for the investigated NCC-treated soil could be that the nanoparticles tend to fill the pore voids and create an aggregated mass that prevented easy imbibing of water, thereby producing a reduction in OMC. A similar OMC reduction was observed for nano-carbon-treated soil investigated by Alsharef et al. (2020) and explained due to filling of the soil pore spaces by the nanomaterial additive. The marginal reduction in MDUW for NCC-treated soil can be attributed to greater resistance offered to the compaction effort arising from the aggregation effect — aggregated soil generally tending to exhibit reduced density (Zhang, 2007). Reduced availability of water and

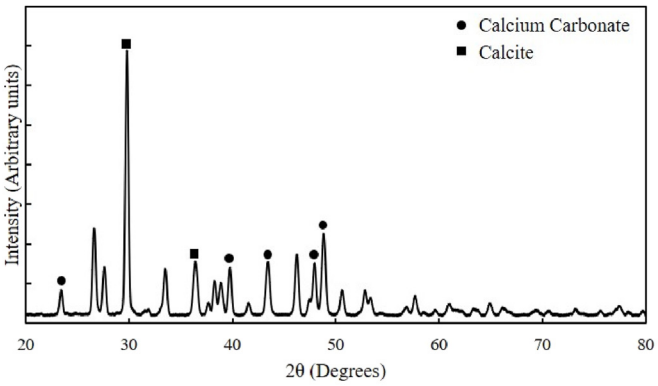

Fig. 3. XRD peaks of the investigated NCC material.

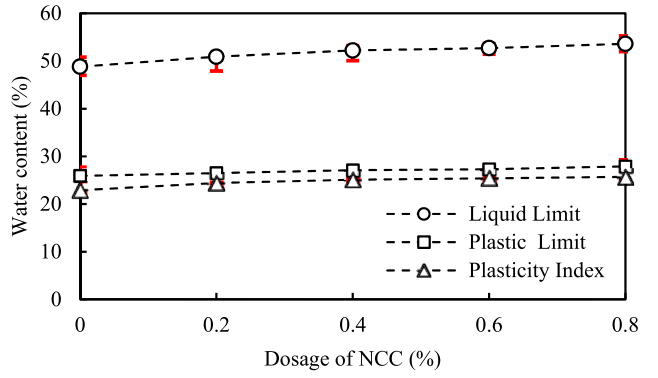

Fig. 4. Variation in plasticity characteristics of NCC-treated soil. All the errors are within 7.5%.

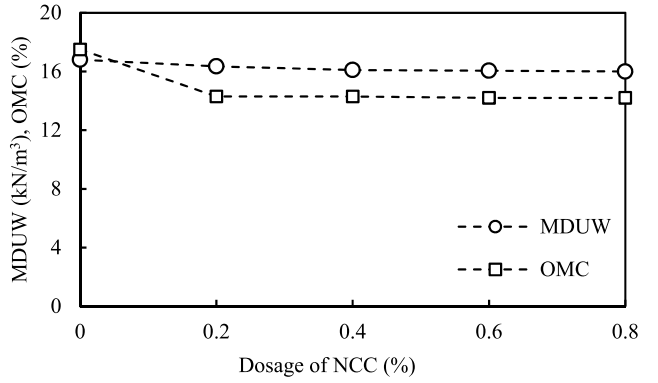

Fig. 5. Variation in MDUW and OMC of untreated and NCC-treated soil.

the higher specific surface area of the $CaCO_3$ nanoparticles caused aggregation of the soil mass. A similar aggregation phenomenon was explained for NS-based concrete preparation in Khaloo et al. (2016) and Mohammed and Adamu (2018).

3.3. Strength characteristics

Treating the soil with NCC additive and subsequent curing of the SP-compacted test specimens greatly improved the UCS for all dosages and each curing period investigated (Fig. 6). Compressed specimens exhibited a brittle nature, with drastic reductions in post-peak UCS for NCC-treated soil. Similar brittle behavior was reported by Ibrahim et al. (2020) on treating clay with limestone powder.

Referring to Fig. 6, the UCS of all NCC-treated soil specimens exceeded that of the untreated soil. For 2-h curing (i.e. 0 d), the untreated soil had a UCS of 172.4 kPa, which increased to a maximum value of 266.7 kPa for 0.4% NCC addition — soil treated with 0.6% and 0.8% additive showed reduced UCS of 237.6 kPa and 234.7 kPa, respectively. Soil treated with 0.4% NCC mobilized progressively higher strengths for 7 d, 14 d, 28 d, 56 d and 90 d curing periods, with UCS of 273.8 kPa, 304.1 kPa, 356 kPa, 392.8 kPa and 506.8 kPa, respectively. Hence, 0.4% NCC addition was identified as the optimum dosage in terms of UCS improvement. The mechanisms of strength improvement are schematically presented in Fig. 7. As pozzolanic reactions are time dependent (Saygili, 2015; El-Mahllawy et al., 2018), strength improvement for the early curing period could be attributed to void filling and particle aggregation, whereas formation of hydration products for longer curing periods would have imparted greater UCS (El-Mahllawy et al., 2018; Choobbasti et al., 2019; Pastor et al., 2019).

Fig. 8 shows the FTIR spectra for the untreated and NCC-treated soils that help in the identification of associated functional group variation. It can be observed that the trends in the presented spectra for the 0.4% NCC-treated and untreated soils remain approximately similar, except for the change in their intensities. The band around 800 cm^{-1} indicates the presence of amorphous silica (El-Mahllawy et al., 2018), whereas the trough around 1030 cm^{-1} indicates the presence of alumino-silicate lattice, arising from the presence of clay minerals (Tinti et al., 2015). The stretching bands around 3400 cm^{-1} denote the stretching of OH from water, indicating the water adsorption by the sample (El-Mahllawy et al., 2018). However, these FTIR spectra alone cannot be used to interpret the soil chemical behavior which must be verified with other supplementary analysis of composition through XRD analysis.

Results of XRD analysis for the untreated and 0.4% NCC-treated soils are presented in Fig. 9. It can be inferred from this figure that a pattern matching CSH is found in the investigated soil sample treated with 0.4% NCC. CSH forms due to the reaction between the calcium ions from the additive and the silicon ions from the clay minerals in the soil (Mohammadi et al., 2021). It should be noted from the XRD pattern that the soil itself contains traces of $CaCO_3$. A field survey revealed the presence of calcite deposits, as white fragments, below the sampled soil stratum. Saygili (2015) reported the effects of marble dust additive on the behavior of clays — the presence of calcium ions from the additive and silica ions from the treated soil leading to the formation, over time, of cementitious products from their pozzolanic reaction. El-Mahllawy et al. (2018) also reported time-dependent CSH and poor crystalline gel

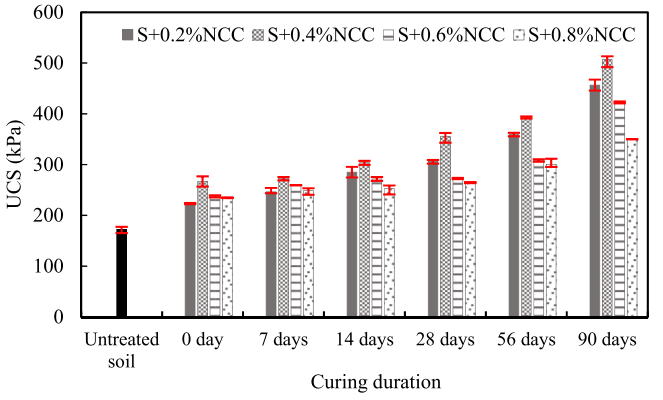

Fig. 6. Strength variation with curing period for NCC-treated soil. All the errors are within 5%.

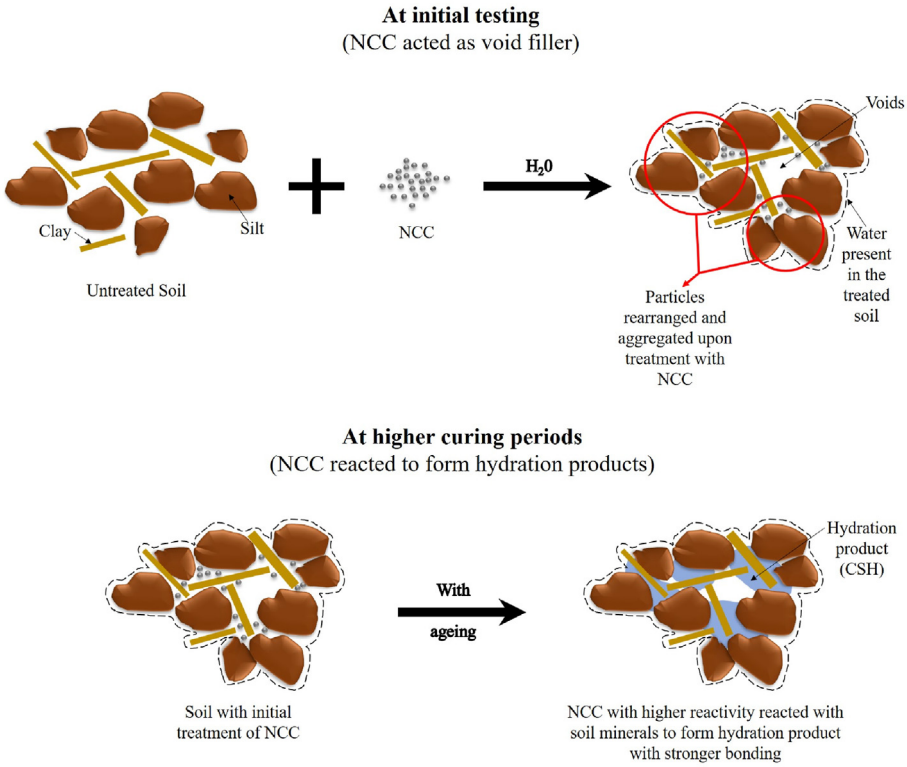

Fig. 7. Strength improvement mechanisms for NCC-treated soil.

formations for calcite and quartz-rich marble waste blended with clayey soil.

In general, calcium carbonate is a strong compound that cannot be easily dissolved in water to dissociate into ions. But in their investigation of NCC-treatment for soil strength enhancement, Mohammadi et al. (2022) stated that the reactivity increases with decreasing particle size of calcium carbonate to nanoscale; the higher reactivity of NCC causes reactions to occur with the clay minerals in the soil leading to CSH gel formation, as given by the following equation:

$$\text{Clay} + \text{nano-CaCO}_3 \rightarrow \text{CSH (gel)} \quad (1)$$

Upon formulating Eq. (1), one obtains

$$\text{SiO}_2 + \text{Ca}^{2+} \xrightarrow{\text{H}_2\text{O}} \text{CaO}\cdot\text{SiO}_2\cdot\text{H}_2\text{O} \quad (2)$$

The reactions in Eqs. (1) and (2) explain the CSH traces observed in the present study for the cured NCC-treated soil.

SEM images captured for the 7-d-cured 0.4% and 0.6% NCC-treated and untreated soils are shown in Fig. 10. The NCC additive initially created additional tiny voids in the soil matrix because of increased particle aggregation, with the gel formation for 7-d curing (Fig. 10b and c) holding the soil particles together, thereby leading to higher UCS mobilization. Also, it can be noted from Fig. 10c that the effect of aggregation is more prominent for 0.6% NCC addition, thereby explaining its reduced UCS compared to that mobilized for 0.4% additive (refer to Fig. 6).

3.4. Permeability characteristics

The average saturated permeability coefficient (k_v) measured from falling-head permeability testing of the fully-saturated

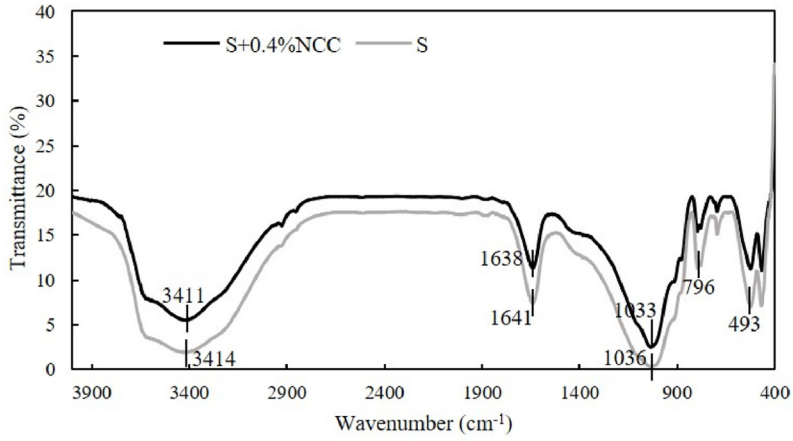

Fig. 8. FTIR patterns of untreated and 0.4% NCC-treated soils.

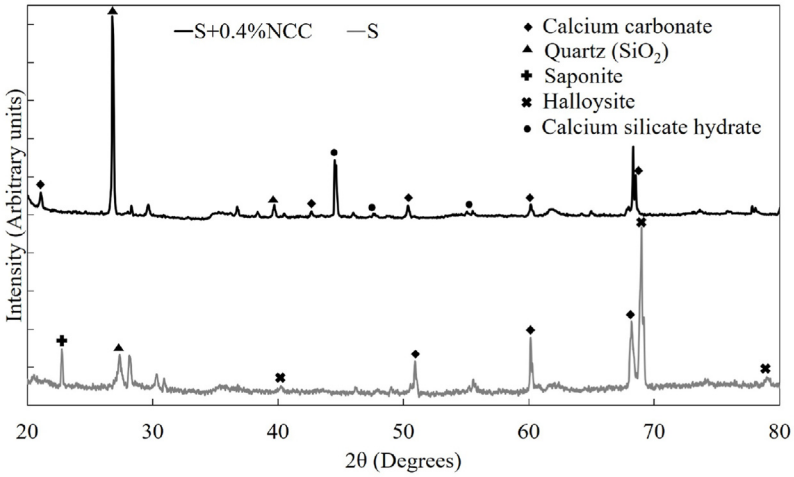

Fig. 9. XRD plots of untreated and 0.4% NCC-treated soils.

untreated soil was 8.8×10^{-10} m/s. The k_v magnitude of the 0.2%–0.8% NCC-treated soils was approximately one order of magnitude greater (Fig. 11). This is consistent with the lower MDUW of 16–16.35 kN/m^3 (and hence higher void ratio) of the NCC-treated soil compared to the untreated soil (16.8 kN/m^3). It is also evident from Fig. 11 that the k_v magnitude of the treated soil marginally increased for up to a dosage of 0.4% NCC, but started to decrease for more additive. For instance, 7-d cured specimens showed k_v values of 10.5×10^{-9} m/s, 17.8×10^{-9} m/s, 14×10^{-9} m/s and 8.6×10^{-9} m/s for 0.2%, 0.4%, 0.6% and 0.8% NCC dosages, respectively. Furthermore, the k_v magnitude showed an exponential reduction with increased curing period. For instance, 0.4% NCC-treated soil showed a reduction in k_v from 15.9×10^{-9} m/s to 13.1×10^{-9} m/s, 10.1×10^{-9} m/s and 8.5×10^{-9} m/s for 14 d, 28 d, 56 d and 90 d curing, respectively. The 90-d-cured 0.8% NCC-treated soil showed the least k_v value of 1.2×10^{-9} m/s, although this was still greater than that for untreated soil (8.8×10^{-10} m/s).

The higher permeability for the early curing period (7 d) could be due to the fact that the NCC additive would have exchanged calcium ions with cations in the soil (Choobbasti et al., 2019) for the fully saturated test specimens. In turn, this would lead to flocculation or agglomeration of soil particles, with greater permeability associated with the flocculated structure. Lower MDUW (i.e. higher void ratio) and absence of hydration product formation in the early curing period would also account for the increased permeability. Hydration product formation with increasing curing period would cause progressive filling of the pore spaces, thereby leading to reduced permeability (Saygili, 2015; El-Mahllawy et al., 2018; Kannan and Sujatha, 2022).

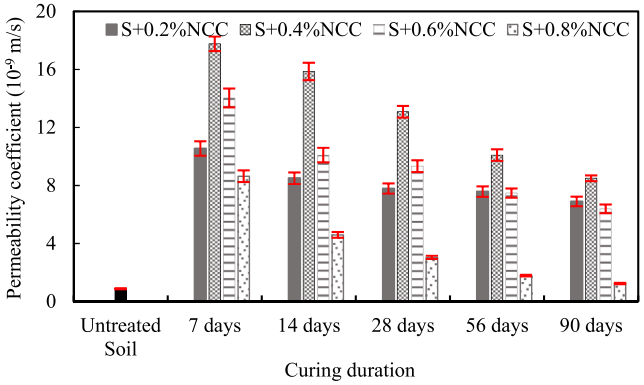

Fig. 11. Falling-head permeability coefficient variation with curing period for NCC-treated soil. All the errors are within 5%.

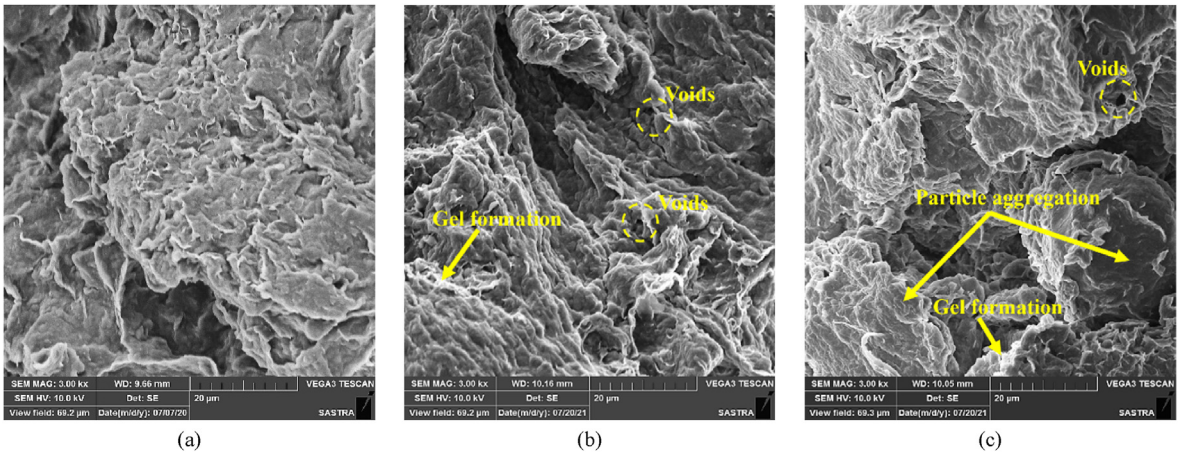

Fig. 10. SEM images for 7-d curing: (a) Untreated soil, (b) 0.4% NCC-treated soil, and (c) 0.6% NCC-treated soil.

Porosity estimation was performed based on analysis of the SEM images shown in Fig. 10. Although this approach is approximate, it can help to proportionately relate the variation in porosity among the various samples. Results from the image processing analysis showed that the untreated soil had a porosity of 13%, which increased to 18.4% and 18.3% porosity for the 0.4% and 0.6% NCC-treated samples, respectively. This indicates that the volume of pore voids increased for 0.4% additive and reduced slightly for the higher 0.6% dosage. In general, porosity holds a proportional relationship with permeability, and this has been reflected in the obtained results.

3.5. Compressibility characteristics

The compressibility properties deduced from consolidation testing of 1-d cured saturated, 0.2%, 0.4% and 0.6% NCC-treated and untreated soils are listed in Table 3. Taylor's square-root-of-time curve-fitting method was adopted for determination of the coefficient of consolidation (c_v), analyzing the lowest and highest applied pressures of σ_v = 9.8 kPa and 313.8 kPa investigated. The compression index (C_c) and swelling/recompression index (C_s) were obtained from the compression curves shown in Fig. 12.

As expected, the c_v magnitude (an indicator of the consolidation rate) deduced for the first load step (9.8 kPa) was significantly greater than that for the final applied load of 313.8 kPa on account of the reducing void ratio with increasing effective stress (see reported c_v for the untreated and NCC-treated soils in Table 3). Compared to the untreated soil and considering a given load step, the results indicate relative increases in c_v for 0.2% and 0.4% NCC additions, with the opposite occurring for 0.6% additive. It is evident from the c_v results that the presence of more pore-void space in the NCC-treated soil (higher void ratio) resulted in a larger sample compression per unit time and thus higher c_v values.

The compression index for 0.2%–0.6% NCC-treated soil remained practically constant at 0.57, substantially below the 0.97 value measured for the untreated soil. Hence, the results in Table 3 indicate that the NCC-treated soil tends to compress at a relatively faster rate, but achieves a comparatively lower compression strain, compared to the untreated soil. A similar reduction in compression index was observed by Mohammadi et al. (2021) for clayey sand treated with NCC additive. The swelling/recompression index (C_s) magnitude reduced for up to 0.4% NCC dosage and then started increasing beyond that. A similar reduction in C_s for up to an optimum dosage, followed by a small increment beyond that, was also observed by Mohammadi et al. (2021) from testing of clayey sand treated with NCC additive.

The k_v magnitude derived from the consolidation test results for the applied pressures of σ_v = 9.8 kPa and 313.8 kPa was found to reduce from 6.45×10^{-10} m/s to 0.51×10^{-10} m/s, 23.37×10^{-10} m/s to 0.66×10^{-10} m/s, 14.66×10^{-10} m/s to 0.57×10^{-10} m/s and 12.75×10^{-10} m/s to 0.52×10^{-10} m/s for the 1-d cured 0%, 2%, 4% and 0.6% NCC-treated samples, respectively. The derived value of 6.45×10^{-10} m/s for the untreated soil under σ_v = 9.8 kPa is in good agreement with the average falling-head k_v value of 8.8×10^{-10} m/s measured for the same soil (see Section 3.4). As expected, both untreated and NCC-treated soils subjected to increasing applied pressure of up to 313.8 kPa exhibited progressively reducing k_v compared to the measured falling-head k_v for the untreated soil. A slight increase in the derived k_v magnitude was observed for 0.2% NCC additive, and it was found to reduce for more additive, following a similar trend to the falling-head k_v results (Fig. 11).

Table 3
Compressibility properties of NCC-treated soil obtained from consolidation testing of 1-d cured samples.

Parameter	Untreated soil	0.2% NCC-treated soil	0.4% NCC-treated soil	0.6% NCC-treated soil
c_v (m^2/year) (σ_v = 9.8 and 313.8 kPa)	1.11 and 0.12	2.13 and 0.42	4.76 and 0.43	1.99 and 0.33
C_c	0.97	0.58	0.57	0.57
C_s	0.043	0.032	0.032	0.037

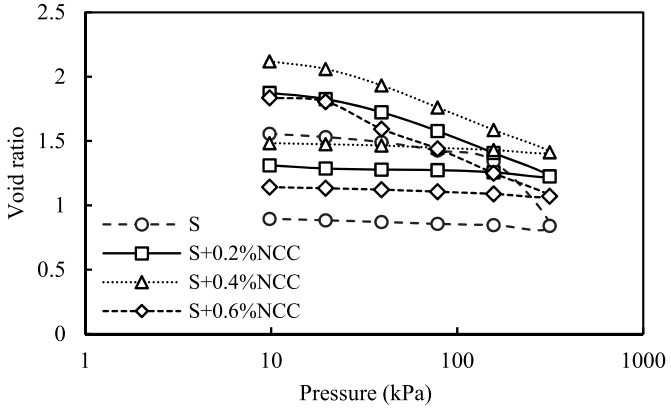

Fig. 12. Compression curves for untreated and NCC-treated soils from consolidation testing of 1-d cured samples.

4. Conclusions

This paper presented some geotechnical engineering properties of low-plasticity organic silt treated with 0.2%, 0.4%, 0.6% and 0.8% NCC additive, investigating curing periods of up to 90 d. The investigated NCC additive range is substantially lower compared to those typically employed for conventional soil stabilization additives (cement and lime). The following results are inferred from the experimental data:

(1) The liquid limit, plastic limit and plasticity index marginally increased for increasing NCC dosage, with the untreated and 0.8% NCC-treated soils having plasticity index values of 22.9% and 25.7%, respectively.
(2) The OMC and MDUW (for SP compaction effort) both experienced modest reductions with increasing NCC dosage — OMC reducing from 17.5% for the untreated soil to 14.3% for 0.2% NCC addition, maintaining approximately the same OMC magnitude for higher dosages.
(3) The UCS of the treated SP-compacted soil showed an optimum dosage of 0.4% NCC addition, with a 55% UCS improvement achieved within 2-h of blending the materials together and a 194% UCS improvement mobilized for 90-d curing, when compared with the untreated soil. The early strength improvement was achieved by void filling, with further strength gains for increased curing occurring because of weak crystalline CSH gel formation.
(4) For NCC-treated soil, the permeability coefficient increased for up to 0.4% additive and decreased thereafter. The treated soil initially showed higher permeability due to the flocculated structure, but the permeability reduced with increased curing for all dosages investigated on account of gel formation.
(5) Compared to the untreated soil, the compression index magnitude decreased for 0.2% NCC addition and then remained approximately constant for higher dosages, whereas the coefficient of consolidation increased for 0.2% and 0.4% additive and then decreased for 0.8% additive. This implies that for the optimum 0.4% NCC dosage (in terms of UCS improvement), the consolidation rate under maintained loading is relatively faster, and the compression magnitude relatively lower, compared to the untreated soil.

The study proposed the use of NCC material as a viable additive for soil stabilization purposes. The general inference of the results is that the strength of the treated soil increased for up to an optimum dosage of 0.4% NCC additive and decreased beyond that, with the same trend observed when considering each curing period investigated. Similarly, the permeability coefficient of the treated soil increased for up to 0.4% NCC additive and then reduced beyond that. However, compared to the untreated soil, the permeability of the NCC-treated soil remained greater, even for the longest curing period of 90-d investigated. Hence, the NCC additive can give effective performance for ground improvement — including, for instance, foundation applications requiring enhanced strength and permeability/drainage properties.

The presented investigation is an elementary step towards alternative nano-additives for soil stabilization purposes. The additive dosage requirement and its effectiveness and reactivity depend on the nature of the treated soil, including chemical constituents and the presence of clay minerals, among other factors. Hence, the authors recommend further investigations of the behavior/properties for other NCC-treated soil types, including application-based field and model studies, which would aid in developing the scope of nano-material-based stabilization treatment considering the present trends.

Declaration of competing interest

The authors declare that they have no known competing financial interests or personal relationships that could have appeared to influence the work reported in this paper.

Acknowledgments

The authors thank the Vice Chancellor and the management of SASTRA Deemed to be University, Thanjavur, India for the support and facilities provided to carry out this work successfully.

References

Ahmadi, H., Shafiee, O., 2019. Experimental comparative study on the performance of nano-SiO_2 and microsilica in stabilization of clay. Eur. Phys. J. Plus 134, 1–14.
Ali Zomorodian, S.M., Shabnam, M., Armina, S., O'Kelly, B.C., 2017. Strength enhancement of clean and kerosene-contaminated sandy lean clay using nanoclay and nanosilica as additives. Appl. Clay Sci. 140, 140–147.
Alsharef, J.M.A., Taha, M.R., Govindasamy, P., Firoozi, A.A., Mansob, R.A.A., 2020. Effect of nanocarbons on physical and mechanical properties of soils. In: Carbon Nanomaterials for Agri-Food and Environmental Applications, Micro and Nano Technologies. Elsevier, pp. 459–485.
Amin, M., Zomorodian, S.M.A., O'Kelly, B.C., 2017. Reducing the hydraulic erosion of sand using microbial-induced carbonate precipitation. Proc. Inst. Civ. Eng. Gr. Improv. 170 (2), 112–122.
Assadi-Langroudi, A., O'Kelly, B.C., Barreto, D., et al., 2022. Recent advances in nature-inspired solutions for ground engineering (NiSE). Int. J. Geosynth. Ground Eng. 8, 3.
ASTM D698-12, 2012. Standard Test Methods for Laboratory Compaction Characteristics of Soil Using Standard Effort (12400 ft-Lbf/ft^3 (600 kN-M/m^3)). ASTM International, West Conshohocken, PA, USA.
ASTM D854-14, 2014. Standard Test Methods for Specific Gravity of Soil Solids by Water Pycnometer. ASTM International, West Conshohocken, PA, USA.
ASTM D2166/D2166M-16, 2016. Standard Test Method for Unconfined Compressive Strength of Cohesive Soil. ASTM International, West Conshohocken, PA, USA.
ASTM D2435/D2435M-11(2020), 2020. Standard Test Methods for One-Dimensional Consolidation Properties of Soils Using Incremental Loading. ASTM International, West Conshohocken, PA, USA.
ASTM D2974-20, 2020. Standard Test Methods for Determining the Water (Moisture) Content, Ash Content, and Organic Material of Peat and Other Organic Soils. ASTM International, West Conshohocken, PA, USA.
ASTM D4318-17, 2017. Standard Test Methods for Liquid Limit, Plastic Limit, and Plasticity Index of Soils. ASTM International, West Conshohocken, PA, USA.
ASTM D5856-15, 2015. Standard Test Methods for Measurement of Hydraulic Conductivity of Porous Materials Using a Rigid Wall Compaction Mould Permeameter. ASTM International, West Conshohocken, PA, USA.
ASTM D5890-19, 2019. Standard Test Method for Swell Index of Clay Mineral Component of Geosynthetic Clay Liners. ASTM International, West Conshohocken, PA, USA.
ASTM D6913/D6913M-17, 2017. Standard Test Methods for Particle-Size Distribution (Gradation) of Soils Using Sieve Analysis. ASTM International, West Conshohocken, PA, USA.
ASTM D7928-21e1, 2021. Standard Test Method for Particle-Size Distribution (Gradation) of Fine-Grained Soils Using the Sedimentation (Hydrometer) Analysis. ASTM International, West Conshohocken, PA, USA.
Baldovino, J.A., Moreira, E.B., Teixeira, W., Izzo, R.L.S., Rose, J.L., 2018. Effects of lime addition on geotechnical properties of sedimentary soil in Curitiba, Brazil. J. Rock Mech. Geotech. Eng. 10, 188–194.
Bazarbekova, A., Shon, C.S., Kissambinova, A., Kim, J.R., Zhang, D., Moon, S.W., 2021. Potential of limestone powder to improve the stabilization of sulfate-contained saline soil. In: Proceedings of the 5th International Conference on New Material and Chemical Industry (NMCI 2020), Xiamen, China.
Cao, G., Wang, Y., 2018. Nanostructures and Nanomaterials: Synthesis, Properties, and Applications, second ed. World Scientific Publishing.
Cardoso, R., Pires, I., Duarte, S.O.D., Monteiro, G.A., 2018. Effects of clay's chemical interactions on biocementation. Appl. Clay Sci. 156, 96–103.
Carmona, J.P.S.F., Oliveira, P.J.V., Lemos, L.J.L., Pedro, A.M.G., 2018. Improvement of a sandy soil by enzymatic calcium carbonate precipitation. Proc. Inst. Civ. Eng. Geotech. Eng. 171 (1), 3–15.
Changizi, F., Haddad, A., 2017. Improving the geotechnical properties of soft clay with nano-silica particles. Proc. Inst. Civ. Eng. Gr. Improv. 170 (2), 62–71.
Choi, S.G., Chang, I., Lee, M., Leem, J.H., Han, J.T., Kwon, T.H., 2020. Review on geotechnical engineering properties of sands treated by microbially induced calcium carbonate precipitation (MICP) and biopolymers. Construct. Build. Mater. 246, 118415.
Choobbasti, A.J., Samakoosh, M.A., Kutanaei, S.S., 2019. Mechanical properties soil stabilized with nano calcium carbonate and reinforced with carpet waste fibers. Construct. Build. Mater. 211, 1094–1104.
El-Mahllawy, M.S., Kandeel, A.M., Latif, M.L.A., El-Nagar, A.M., 2018. The feasibility of using marble cutting waste in a sustainable building clay industry. Recycling 3 (3), 1–13.
Emmanuel, E., Lau, C.C., Anggraini, V., Pasbakhsh, P., 2019. Stabilization of a soft marine clay using halloysite nanotubes: a multi-scale approach. Appl. Clay Sci. 173, 65–78.
Ezeakacha, C.P., Rabbani, A., Salehi, S., Ghalambor, A., 2018. Integrated image processing and computational techniques to characterize formation damage. In: SPE International Conference and Exhibition on Formation Damage Control, Lafayette. Louisiana, USA.
Ghasabkolaei, N., Choobbasti, A.J., Roshan, N., Ghasemi, S.E., 2017. Geotechnical properties of the soils modified with nanomaterials: a comprehensive review. Arch. Civ. Mech. Eng. 17 (3), 639–650.
Gutiérrez, S.A., Caneghem, V.J., Martínez, C.J.B., Vandecasteele, C., 2012. Evaluation of the environmental performance of lime production in Cuba. J. Clean. Prod. 31, 126–136.
Ibrahim, H.H., Alshkane, Y.M., Mawlood, Y.I., Noori, K.M.G., Hasan, A.M., 2020. Improving the geotechnical properties of high expansive clay using limestone powder. Innov. Infrastruct. Solut. 5, 112.
IS2720-40, 1997. Methods of Test for Soils, Part 40: Determination of Free Swell Index of Soils. Bureau of Indian Standards, New Delhi, India.
Kannan, K., Bindu, J., Vinod, P., 2020. Engineering behaviour of MICP treated marine clays. Mar. Georesour. Geotechnol. 38, 761–769.
Kannan, G., Sujatha, E.R., 2021. A review on the choice of nano-silica as soil stabilizer. Silicon. https://doi.org/10.1007/s12633-021-01455-z.
Kannan, G., Sujatha, E.R., 2022. Geotechnical behaviour of nano-silica stabilized organic soil. Geomech. Eng. 28 (3), 239–253.
Khalid, N., Mukri, M., Kamarudin, F., Ghani, A.H.A., Arshad, M.F., Sidek, N., Jalani, A.Z.A., Bilong, B., 2015. Effect of nanoclay in soft soil stabilization. In: Hassan, R., Yusoff, M., Alisibramulisi, A., Amin, N.M., Ismail, Z. (Eds.), Proceedings of the International Civil and Infrastructure Engineering Conference 2014. Springer Singapore, Singapore, pp. 905–914.
Khaloo, A., Mobini, M.H., Hosseini, P., 2016. Influence of different types of nano-SiO_2 particles on properties of high-performance concrete. Construct. Build. Mater. 113, 188–201.
Konstantinou, C., Biscontin, G., Jiang, N.J., Soga, K., 2021. Application of microbially induced carbonate precipitation to form bio-cemented artificial sandstone. J. Rock Mech. Geotech. Eng. 13, 579–592.
Majeed, Z.H., Taha, M.R., 2013. A review of stabilization of soils by using nanomaterials. Aust. J. Basic. Appl. Sci. 7 (2), 576–581.
Mohammadi, M., Khodaparast, M., Rajabi, A.M., 2021. Effect of nano calcium carbonate (nano $CaCO_3$) on the strength and consolidation properties of clayey sand soil. Road Mater. Pavement Des. https://doi.org/10.1080/14680629.2021.1976255.
Mohammadi, M., Rajabi, A.M., Khodaparast, M., 2022. Experimental and numerical evaluation of the effect of nano calcium carbonate on geotechnical properties of clayey sand soil. KSCE J. Civ. Eng. 26, 35–46.
Mohammed, B.S., Adamu, M., 2018. Mechanical performance of roller compacted concrete pavement containing crumb rubber and nano silica. Construct. Build. Mater. 159, 234–251.
Morales, L., Garzón, E., Romero, E., Sánchez-Soto, P.J., 2019. Microbiological induced carbonate ($CaCO_3$) precipitation using clay phyllites to replace chemical stabilizers (cement or lime). Appl. Clay Sci. 174, 15–28.

Mujah, D., Cheng, L., Shahin, M.A., 2019. Microstructural and geomechanical study on biocemented sand for optimization of MICP process. J. Mater. Civ. Eng. 31 (4), 04019025.
Park, K., Jun, S., Kim, D., 2014. Effect of strength enhancement of soil treated with environment-friendly calcium carbonate powder. Sci. World J. 2014, 526491.
Pastor, J.L., Tomás, R., Cano, M., Riquelme, A., Gutiérrez, E., 2019. Evaluation of the improvement effect of limestone powder waste in the stabilization of swelling clayey soil. Sustain. Times 11 (3), 679.
Rabbani, A., Salehi, S., 2017. Dynamic modeling of the formation damage and mud cake deposition using filtration theories coupled with SEM image processing. J. Nat. Gas Sci. Eng. 42, 157–168.
Rahman, I.A., Padavettan, V., 2012. Synthesis, properties, and applications of polymeric nanocomposites. J. Nanomater. 2012, 132424.
Rahman, M.M., Hora, R.N., Ahenkorah, I., Beecham, S., Karim, M.R., Iqbal, A., 2020. State-of-the-art review of microbial-induced calcite precipitation and its sustainability in engineering applications. Sustain. Times 12 (15), 6281.
Rebata-Landa, V., 2007. Microbial Activity in Sediments: Effects on Soil Behavior. PhD Thesis. Georgia Institute of Technology, Atlanta, GA, USA.
Saygili, A., 2015. Use of waste marble dust for stabilization of clayey soil. Mat. Sci. 21 (4), 601–606.
Shahrokhi-Shahraki, R., Zomorodian, S.M.A., Niazi, A., O'Kelly, B.C., 2015. Improving sand with microbial-induced carbonate precipitation. Proc. Inst. Civ. Eng. Gr. Improv. 168 (3), 217–230.
Soundara, B., Kulanthaivel, P., Nithipandian, S., Soundaryan, V., 2020. A critical review on soil stabilization using bacteria. In: Proceedings of the 1st International Conference on Sustainable Infrastructure with Smart Technology for Energy and Environmental Management (FIC-SISTEEM-2020), Tamil Nadu, India.
Taha, M.R., Taha, O.M.E., 2012. Influence of nanomaterial on the expansive and shrinkage soil behavior. J. Nanoparticle Res. 14, 1190.
Tinti, A., Tugnoli, V., Bonora, S., Francioso, O., 2015. Recent applications of vibrational mid-infrared (IR) spectroscopy for studying soil components: a review. J. Cent. Eur. Agric. 16, 1–22.
Wu, Z., Khayat, K.H., Shi, C., 2017. Effect of nano-SiO2 particles and curing time on development of fiber-matrix bond properties and microstructure of ultra-high strength concrete. Cement Concr. Res. 95, 247–256.
Zhang, G., 2007. Soil nanoparticles and their influence on engineering properties of soils. In: Geo-Denver 2007. ASCE, Reston, VA, USA, pp. 1–13.
Zhao, Q., Li, L., Li, C., Li, M., 2014. Factors affecting improvement of engineering properties of MICP-treated soil catalyzed by bacteria and urease. J. Mater. Civ. Eng. 26 (12), 04014094.
Zomorodian, S.M.A., Soleymani, A., O'Kelly, B.C., 2019a. Briefing: improving erosion resistance of sand using nano-silica additive. Proc. Inst. Civ. Eng. Gr. Improv. 172 (1), 3–11.
Zomorodian, S.M.A., Ghaffari, H., O'Kelly, B.C., 2019b. Stabilisation of crustal sand layer using biocementation technique for wind erosion control. Aeolian Res. 40, 34–41.
Zomorodian, S.M.A., Moghispoor, S., O'Kelly, B.C., Babaei, S.S., 2020. Improving internal erosion resistance of silty sand using additives. Dams Reservoirs 30 (1), 29–41.

Govindarajan Kannan completed his bachelor's degree in Civil Engineering in 2015 from SASTRA Deemed to be University, Thanjavur. He obtained his master degree in Soil Mechanics and Foundation Engineering from College of Engineering, Guindy in 2018. Currently he is pursuing his full-time doctoral research on nano-biomaterials based ground improvement techniques at the Centre for Advanced Research in Environment under the guidance of Prof. Sujatha Evangelin Ramani, SASTRA Deemed to be University. His research interests include sustainable ground improvement techniques, advanced foundation analysis using finite element method (FEM), sustainable building materials, biopolymer and nano-additive characterization and their applications in geotechnical engineering.